Adsorption/desorption characteristics for methane, nitrogen and carbon dioxide of coal samples from Southeast Qinshui Basin, China

Fengde Zhou[1,2*], Furqan Hussain[1], Zhenghuai Guo[1], Sefer Yanici[1] and Yildiray Cinar[1]

[1]School of Petroleum Engineering, University of New South Wales, Sydney, NSW 2052, Australia

[2]Key Laboratory of Tectonics and Petroleum Resources (China University of Geosciences), Ministry of Education, Wuhan 430074, China

**Author for Corresponding. Email: f.zhou@unsw.edu.au; fdzhou@cug.edu.cn*

(Received 11 August 2012; accepted 16 February 2013)

Abstract

This paper presents an experimental and modelling study of the adsorption/desorption of pure gases CH_4, CO_2 and N_2 and their binary and ternary mixtures on coal samples obtained from southeast Qinshui Basin, China. Results show that the adsorbed amounts of N_2, CH_4 and CO_2 have approximate ratios of 1.0:1.3:2.4, respectively. No significant hysteresis from adsorption to desorption is observed for pure N_2 and CH_4 whereas significant hysteresis is measured for CO_2 in CO_2-CH_4 and CO_2-CH_4-N_2 mixtures and CH_4 in the N_2-CH_4 mixture. The experimental observations are modelled using three different models, namely the extended Langmuir (EL), the Langmuir-based ideal adsorbed solution (L-IAS) and the Dubinlin-Radushkevich-based ideal adsorbed solution (D-R-IAS). The models predict well the experimental observations for desorption tests. But the measurements for the low adsorbate capacity in binary and ternary mixtures are overestimated by the prediction models. It is found that the EL model predicts the CO_2-CH_4 desorption test better while the D-R-IAS model is the best model for the CO_2-CH_4-N_2 adsorption.

Keywords: Adsorption, Desorption, Gas mixture, Coalbed methane, Qinshui Basin

1. INTRODUCTION

The process of enhanced coalbed methane recovery (ECBM) strongly depends on the type of injection gas composition, e.g. pure/a mixture of CO_2 and N_2 or flue gas (Stevens *et al*., 1998; Mazumder and Wolf, 2008; Connell *et al*., 2011). When CO_2 is injected, it is adsorbed by coal more than CH_4 through which CH_4 is displaced from coal. The ECBM mechanism with N_2 as injectant relies on lowering the partial

pressure of CH_4 in the cleat system and thereby making CH_4 to be desorbed from coal (Puri and Yee, 1990). Both gases offer technical and economical advantages and disadvantages. For example, CO_2 injection can help delay the breakthrough time and reduce greenhouse gas emissions to the atmosphere for which project may benefit from additional revenue from carbon credits. But, at the same time, it can also cause coal to swell which, in turn, decreases coal permeability (Shi and Durucan, 2005; Mazumder *et al*., 2006). As a consequence, the required economic injection rate may not be obtained. On the contrary, N_2 injection increases coal permeability (Mitra *et al*., 2008) which enhances the CH_4 production rate at early stage. At the later stage, however, N_2 breakthroughs at producers earlier compared to CO_2 which results in a lower ultimate recovery. Moreover, there is no credit for storing N_2 which may bring additional costs to the project in comparison to CO_2 injection (Zhou *et al*., 2011). Hence, all these features of ECBM need to be understood properly before any project. During these processes, adsorption/desorption characteristics play an important role in determining which gas or gas mixture should be used. Hence, an accurate understanding of the adsorption/desorption competition between pure and mixture gases in a specific coal is essential for an accurate design of ECBM.

Adsorption/desorption characteristics of pure or a mixture gas are generally measured using laboratory tests (Stevenson *et al*., 1991; Hall *et al*., 1994; Yu *et al*., 2008; Gruszkiewicz *et al*., 2009; Pini *et al*., 2009, 2010). The size of coal sample used in experiments is reported to range from decades of microns to several centimetres (Yu *et al*., 2008; Kelemen and Kwiatek, 2009; Papanicolaou *et al*., 2009; Gruszkiewicz *et al*., 2009; Wang *et al*., 2010). Besides, it is known that using crushed coal in experiments can reduce the experimental time remarkably (Gruszkiewicz *et al*., 2009). Other important parameters that play important role in the adsorption/desorption of gases on/from coal are coal rank (Schepers *et al*., 2010; Ding *et al*., 2011), moisture (Joubert *et al*., 1973; Goodman *et al*., 2007) and shrinkage/swelling (Hema *et al*., 2009; Majewska *et al*., 2010; Wang *et al*., 2010; Battistutta *et al*., 2010).

For pure gas adsorption in coal, it is known that coal absorbs more CO_2 than CH_4 and CH_4 more than N_2 (Pini *et al*., 2009). Because ECBM includes adsorption/desorption of multiple gases it is also needed to understand the adsorption/desorption characteristics of gas mixtures. However, gas mixture experiments are rather time consuming as they require the measurement of gas compositions. An alternative proposed solution is the use of predictive models for adsorption/desorption of binary/ternary gases. Three prediction models, namely the extended Langmuir (EL), the ideal adsorbed solution (IAS), and the real adsorbed solution (RAS) models, have been widely used to estimate binary/ternary gas adsorption characteristics of coal from its pure isotherm data (Myers and Prausnitz, 1965; Talu and Zwiebel, 1984; O'Brien and Myers, 1985; Gamba *et al*., 1989; Hall *et al*., 1994; Dreisbach *et al*., 1999; Yu *et al*., 2008). Stevenson *et al*. (1991) noted that the RAS model is not always better than the IAS model, in particular when the mixed gas has higher CO_2 or N_2 concentrations.

The motivation for this study has come from the necessity of the knowledge of adsorption/desorption characteristics in a techno-economic modelling of the ECBM potential of a coalbed methane (CBM) field in South Qinshui Basin (Zhou *et al*.,

2012). No reported data of adsorption/desorption for the study area was available for the project and hence series of laboratory tests were carried out for pure and binary/ternary gas mixtures. The experimental results are presented in this paper. Then the predictions made by three different models proposed in the literature are compared.

2. EXPERIMENTAL PROCEDURE

2.1. Sample preparation

The coal sample used in this study was collected from a nearby coal mine – Duanshi Coal Mine – which is producing coal from the same seam (seam No.3) as the Shizhuang coalbed methane district, south Qinshui Basin in China. The average composition of the produced gas was 99.35% CH_4, 0.14% N_2 and 0.5% CO_2, measured on no-air base using 12 gas samples from the study area. The H_2S content was less than 1mg/m^3. The coal sample was first crashed to a particle size ranging from 0.25 to 0.5 mm (60 mesh to 35 mesh). Then the sample was dried at 60 ˚C for two hours. All calibration and experimental tests were carried out at a constant temperature of 25 ˚C. The pure gases used in the experiments were obtained from Coregas^{TM} Australia.

2.2. Experimental apparatus and calibration

Figure 1 shows the apparatus used for volumetric adsorption measurements. The apparatus consisted of stainless steel cells of three different volumes (two as reference cells “RC” and one as sample cell “SC”), four gas cylinders, a buffer bottle and three pressure transducers with different maximum pressures, 34 MPa (5,000 psi), 6.9 MPa (1,000 psi) and 3.4 MPa (500 psi). A syringe and a vial were used to collect gas at the atmospheric pressure and input to a gas chromatograph (GC).

The volumetric method was used (Stevenson *et al*., 1991; Yu *et al*., 2008). The system was first vacuumed down to a pressure of 0.7 kPa (0.1 psi). Then the system was filled with pure gas in the RC and connected to the SC while keeping the pressure

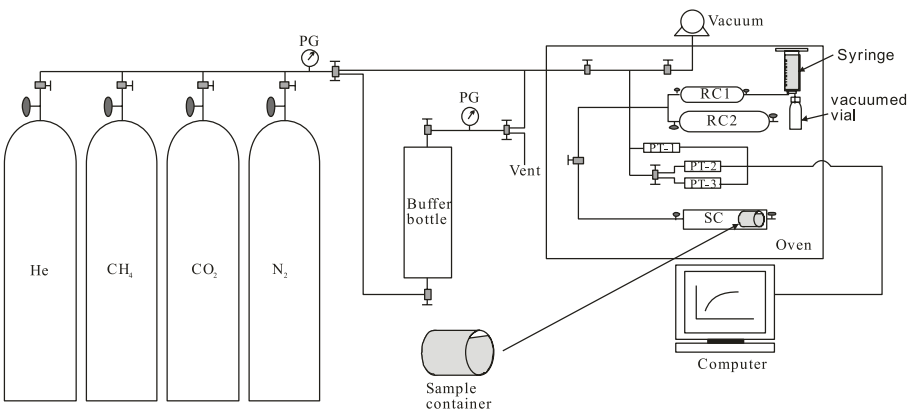

Figure 1. Schematic diagram of test apparatus, RC=Reference cell, SC=Sample cell, PT=Pressure Transducer, PG=Pressure gauge.

constant at 0.7 kPa (0.1 psi) for 30 min. The two equilibrium pressures for each adsorption point were recorded automatically by a personal computer. The RC was then disconnected from the SC and was introduced with more gas to repeat the test at a higher equilibrium pressure. The process was then reversed to determine the desorption points. The same experimental procedure was applied for gas mixtures with the only difference being testing the gas composition in the RC at equilibrium before and after connecting to the SC.

The volumes of the RC and SC were calibrated using helium and a cubic stainless steel of known volume. Two equilibriums with and without the cubic stainless steel were conducted to identify the volumes of the RC and SC using the following two equations based on the Boyle's Law:

$$P_1 \cdot V_{RC} + P_2 \cdot V_{SC} = P_t \cdot (V_{RC} + V_{SC}) \tag{1}$$

$$P_1' \cdot V_{RC} + P_2' \cdot (V_{SC} - V_{steel}) = P_t' \cdot (V_{RC} + V_{SC} - V_{steel}) \tag{2}$$

where P_1 and P_1' are the pressures in the RC before connecting to the SC, P_2 and P_2' are the pressures in the SC before being connected with the RC, P_t and P_t' are the equilibrium pressures after the connection of the RC and SC. The repeats of three times showed an acceptable reproducibility of the measurements with a deviation of less than 2%.

With a similar process, the sample grain volume was determined using

$$P_1'' \cdot V_{RC} + P_2'' \cdot (V_{SC} - V_{sample}) = P_t'' \cdot (V_{RC} + V_{SC} - V_{sample}) \tag{3}$$

where P_1'' is the pressure in the RC before connecting to the SC and P_2'' is the pressure in the SC before being connected with the RC.

The calibrated volume of the SC was 181.97 cm^3, RC-1 was 75.81 cm^3, RC-2 was 144.02 cm^3, PT-1 was 1.27 cm^3, PT-2 was 6.40 cm^3 and PT-3 was 8.85 cm^3. The weight and volume of the sample were 66.74 g and 46.66 cm^3, respectively. The calculated sample density was 1.43 g/cm^3.

3. BASIC CALCULATION PROCEDURES

3.1. Pure gas adsorption test and calculations

The adsorption volume of pure gas at any discrete step can be calculated using the following equations (Hall *et al*., 1994) -

$$\Delta n_{ads} = \left[\left(\frac{P_1}{Z_{P1}} - \frac{P_t}{Z_{Pt}} \right) V_{RC} + \frac{P_2}{Z_{P2}} (V_{SC} - V_{sample}) - \frac{P_t}{Z_{Pt}} (V_{SC} - V_{sample}) \right] \frac{1}{W_{coal} RT} \tag{4}$$

$$n_{ads-i} = \Delta n_{ads_1} + \Delta n_{ads_2} + \Delta n_{ads_3} + ... + \Delta n_{ads_i} \quad (5)$$

where P_1 is the pressure in the RC before connected to the SC, P_2 is the pressure in the SC before connected to the RC, P_t is the equilibrium pressure after the SC is connected with the RC, Z_t is the total compressibility at the corresponding pressure and temperature, T_{atm}= 273.15 ˚K, P_{atm}= 101.325 kPa, W_{coal} is the dry sample weight and R is the universal gas constant. The equations for Z are given in the appendix.

Eq. 5 gives Gibbs adsorption/desorption data where the adsorbate volume is neglected (Clarkson and Bustin, 2000). The absolute adsorption/desorption data are calculated using the following equation (Hall *et al*., 1994)-

$$n_{abs} = n_{Gib} \cdot \rho_{g-ads} / (\rho_{g-ads} - \rho_{g-gas}) \quad (6)$$

where n is the adsorption/desorption volume, ρ is the density and subscripts *abs*, *Gib*, *g-ads* and *g-gas* represent *absolute*, *Gibbs*, *adsorbate gas* and *gaseous gas*, respectively. In this study, the adsorbate density was determined by the Ono-Kondo model. The adsorbate densities of CH_4, CO_2 and N_2 are 0.345 g/cm^3, 0.701 g/cm^3 and 0.996 g/cm^3, respectively (Sudibandriyo *et al*., 2003).

3.2. Mixed gas adsorption test and calculations

The adsorption tests for the gas mixtures require the gas mixture composition. We used Agilent 7890 Gas Chromatograph (GC) with column HP-Plot Q to determine gas compositions. Table 1 shows the parameters for GC. The calibrations with pure gases showed that the retention times of N_2, CH_4 and CO_2 were about 1.72, 1.87, and 2.50 min, respectively.

The partial pressure, compressibility factor and volume occupied by the adsorbate are determined from -

$$P_i = P \cdot y_i \quad (7)$$

$$Z_p = \sum_{i=1}^{n} Z_{i-p} y_{i-p} \quad (8)$$

$$V_a = \sum_{i=1}^{n} V_{ai} \cdot y_i \quad (9)$$

Table 1. Gas chromatograph setting parameters with column HP-Plot Q.

Carrier gas	Oven	Injection	Detector
Helium, 34.5 kPa (5 psi), flow rate at 8.3mL/min	35˚C, isothermal	100µL syringe, split ratio 1:1	TCD, 200˚C

where P is the total pressure of gas mixture, y_i is the mole fraction of composition i in the gas phase which is determined by GC.

Experimental data of pressure, calibrated volumes of the RC, SC and coal sample, sample weight and density are used to calculate the adsorptions of pure and mixed gases using the Boyle's law and real gas law with the Soave-Redlich-Kwong equation of state (SRK-EOS) (see the appendix for details).

3.3. Prediction models

3.3.1. Pure-component adsorption isotherm

In order to simulate pure or mixed gas adsorption in coal seam, the experimental discrete data must be matched with an isotherm model. There are three linearized isotherm models, namely the Langmuir, the Freundlich and the Dubinin-Radushkevich (D-R) isotherms (Richter *et al*., 1989; Yu *et al*., 2008; Wood, 2002). The Freundlich isotherm is inadequate in predicting capacities for unmeasured vapours (Wood, 2002). Therefore, only the Langmuir and D-R isotherms were used in this study. The equations are given by -

Langmuir isotherm:
$$q = \frac{V_{L-i} bp}{1 + bp} \tag{10}$$

D-R isotherm:
$$q = V_D \exp\left\{ -D\left[\ln\left(\frac{p_s}{p}\right) \right]^2 \right\} \tag{11}$$

where $V_{L\text{-}i}$ is the Langmuir volume for component i, b is the Langmuir constant, P is the pressure for the gaseous phase, V_D is the maximum amount adsorbed, D is the D-R constant, P_s is the saturation pressure and p is the pressure.

3.3.2. Extended Langmuir model

The Extended Langmuir (EL) model is a simple approach used widely to predict the mixed gas adsorption (Hall *et al*., 1994). The equations are given by -

$$q_i = V_{L,i} \frac{b_i p_i}{1 + \sum b_j p_j} \tag{12}$$

$$p_i = p_t y_i \tag{13}$$

where $V_{L,i}$ is the Langmuir volume for component i, y_i is the gas fraction of component i in the gaseous phase, b_i is the Langmuir constant for component i and P_t is the total pressure for the gas phase.

3.3.3. Ideal adsorbed solution models

The ideal adsorbed solution (IAS) theory is based on the thermodynamic equilibrium. The theory predicts multi-component adsorption from pure gas isotherms (Richter *et al*., 1989). The key of an IAS model is the calculation of reduced spreading pressure. Myers and Prausnitz (1965) assumed that the reduced spreading pressures (π_i^*) of the components in a gas mixture are equal to the reduced spreading pressure (π^*) of the mixture. The following equations are used to calculate reduced spreading pressures -

$$\pi_i^* = \frac{\pi_i A}{RT} = \int_0^{p_{i0}(\pi)} \frac{q_i}{p_i} dp_i \tag{14}$$

$$\pi_1^* = \pi_2^* = ... = \pi_n^* = \pi^* \tag{15}$$

where A is the specific surface area, R is the universal gas constant, T is the temperature, $p_{i,0}$ is the pressure of single component i, q_i is the adsorption isotherm of component i and p_i is the partial pressure of component i.

The relationship between gas mole fractions in the gas phase (y_i) and in the adsorbed phase (x_i) is described by the Raoult's law for the vapor-liquid equilibrium -

$$py_i = p_{i,0}(\pi)x_i \tag{16}$$

where p is the total pressure in the gas phase. Both the total mole fractions of the components in the gas (y_i) and adsorbed phases (x_i) are equal to 1 -

$$\sum_{i=1}^{n} x_i = 1 \tag{17}$$

$$\sum_{i=1}^{n} y_i = 1 \tag{18}$$

The total adsorbed gas, q_t, can then be calculated by -

$$\frac{1}{q_t} = \sum_{i=1}^{n} \frac{x_i}{q_{i,0}} \tag{19}$$

$$q_i = q_t x_i \tag{20}$$

where $q_{i,0}$ is calculated by the pure gas isotherm equation at $P_{i,0}$. $P_{i,0}$ is obtained by

solving simultaneously Eqs. 15 and 16 and one of the following models for the reduced spreading pressure (Richter *et al*., 1989):

Langmuir isotherm: $$\pi_i^* = V_{L,i} \ln(1 + bp_{i,0}(\pi)) \tag{21}$$

D-R isotherm: $$\pi_i^* \approx \frac{V_{D,i}\pi^{1/2}}{2D_i^{1/2}} erfc\left[D_i^{1/2} \ln(\frac{p_{s,i}}{p_{i,0}}) \right] \tag{22}$$

where $V_{L,i}$ is the Langmuir volume of component i, $V_{D,i}$ is the maximum adsorption for component i, D_i is the D-R constant for component i, $P_{s,i}$ is the saturation pressure for component i and *erfc* is the error function which is given by -

$$erfc(x) = \frac{2}{\sqrt{\pi}}(x - \frac{x^3}{3} + \frac{x^5}{10} - \frac{x^7}{42} + \frac{x^9}{216} - ...) \tag{23}$$

4. RESULTS AND DISCUSSION

4.1. Pure gas adsorption tests

The procedure includes first injecting CH_4 into the RC, then connecting the RC and SC and finally recording the pressure variation. If the variation of pressure is less than 0.7 kPa (0.1 psi) within 30 min, the pressure is considered to be the equivalent pressure. Then the procedure is repeated by introducing more gas into the SC. After the equivalent pressure is obtained, the compressibility factor is then calculated using the SRK EOS. Finally the adsorption amount is calculated using the equations given in the methodology section.

Figure 2 shows the experimental results for adsorption and desorption of pure gases on coal samples. The adsorption capacity sequence is CO_2, CH_4 and N_2 from high to low. The relative adsorbed amount of N_2, CH_4 and CO_2 has an approximate ratio of 1.0:1.3:2.4. There are no significant hysteresis effects in pure N_2 and CH_4 adsorption and desorption cycles, but there is a clear hysteresis effect in the CO_2 adsorption/desorption cycle. Tang *et al*. (2005) and Jessen *et al*. (2008) reported a coal which absorbs almost three times as much CO_2 as CH_4 and exhibits significant hysteresis among pure components adsorption and desorption isotherms. It is observed that the adsorption amount of CO_2 at the first desorption point is higher than that at the last adsorption point. Dutta *et al*. (2011) also reported similar observations when they studied a set of Indian coals. This is because the density of CO_2 decreases as pressure decreases which causes more gaseous CO_2 in the system to be adsorbed.

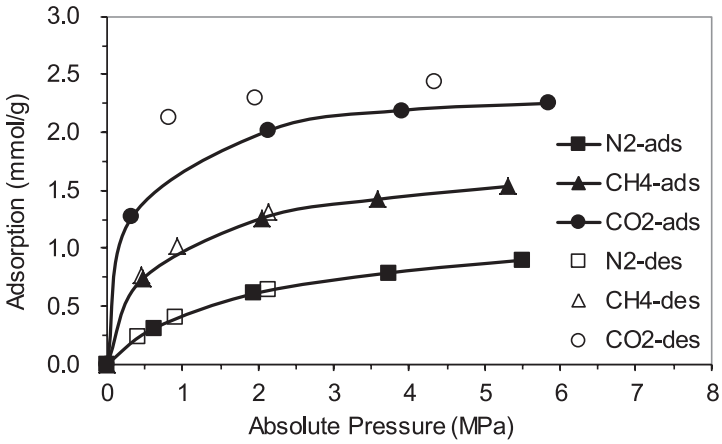

Figure 2. Experimental results of adsorption (ads) and desorption (des) of pure gases of CH_4, CO_2 and N_2.

4.2. Adsorption/desorption equilibrium time

Figure 3 shows the equilibrium times for the adsorption/desorption tests. The pressure difference shown on the x-axis represents the pressure in the RC before connecting the RC and SC minus the equilibrium pressure after connecting the RC and SC. Results show that the equilibrium time increases with the increasing pressure difference for pressures lower than 2 MPa (300 psi) and decreases for pressures higher than 2 MPa (300 psi).

4.3. Binary and ternary gas adsorption tests

The experimental results for the adsorption of binary and ternary gas mixtures are shown in Figure 4. The measured molar fraction of N_2 was affected by air when measured using GC. A standard deviation of 0.01 was therefore used in error

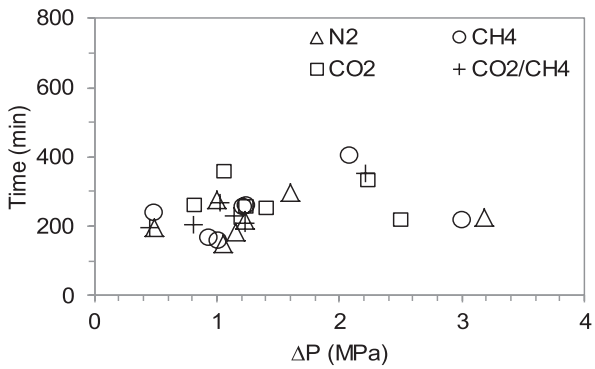

Figure 3. Adsorption/desorption equilibrium times against the difference between the feed gas pressure and equilibrium pressure.

calculation for mixtures CH_4-N_2 and CO_2-CH_4-N_2. We used Oracle Crystal Ball™ to calculate the error ranges and assign P_{90} as the minimum and P_{10} as the maximum values.

Figure 4a shows the total gas adsorption for the gas mixture of CH_4-N_2. It demonstrates that the sample has a stronger adsorption capacity for CH_4 than N_2. The total adsorption has hysteresis effects during the cycle from adsorption to desorption. The hysteresis is different from pure N_2 or CH_4 adsorption and desorption because this is caused by the displacement of CH_4 for N_2 when desorption occurs.

The adsorption/desorption with mixed CO_2-CH_4 as the adsorbed gas shows similar characteristics to the mixed CH_4-N_2. But the hysteresis of CO_2 over CH_4 is stronger than that of CH_4 over N_2 (Fig. 4b). CO_2 desorbs more CH_4 when pressure decreases.

The adsorption/desorption of mixed CO_2-CH_4-N_2 shows that the coal sample has lower adsorption capacity for N_2 than CH_4 than CO_2 (Fig. 4c). CO_2 and CH_4 displace N_2 during the desorption process.

4.4. Modelling experimental results using three isotherm models

Because all the models are based on the pure gas adsorption isotherm, we first attempt to fit the experimental pure gas adsorption with the Langmuir and D-R IAS models. Figure 5a shows the comparison of experimental adsorption results and the best-fit

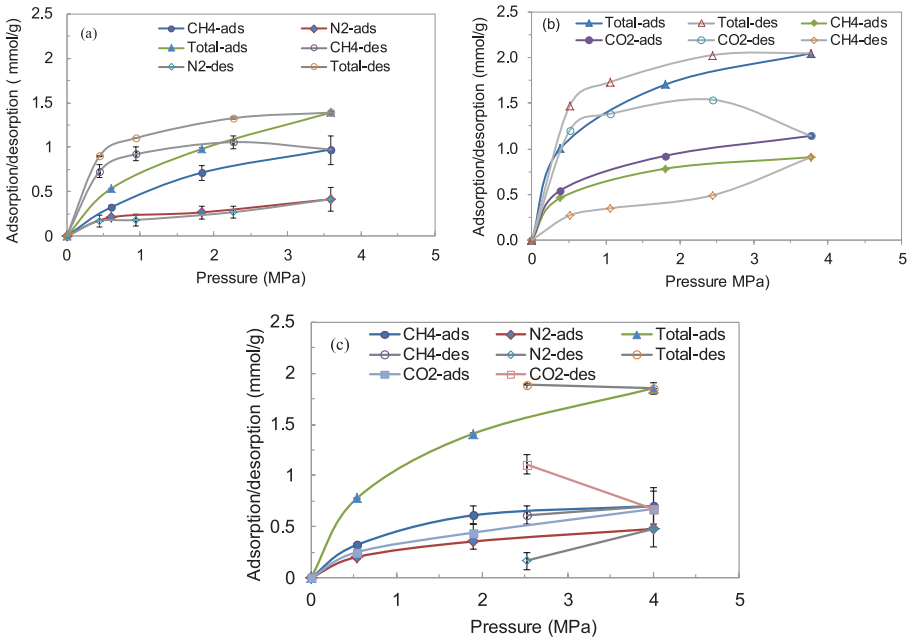

Figure 4. Comparison of adsorption/desorption results of binary and ternary gas mixtures with pure gas adsorption isotherms. (a) N_2-CH_4 mixture, (b) CO_2-CH_4 mixture, (c) CO_2-CH_4 -N_2 mixture.

Langmuir and D-R curves for CO_2, CH_4 and N_2. Figure 5b shows the comparison of experimental desorption results and the best-fit Langmuir and D-R curves for CO_2, CH_4 and N_2. The Langmuir and D-R curves are fitted by experimental data using the least-squares regression method. The fitting parameters for adsorption and desorption are given in Tables 2 and 3, respectively. The data shows that the D-R model has a lower absolute error for fitting the experimental data for CH_4, CO_2 and N_2 adsorption than the Langmuir model.

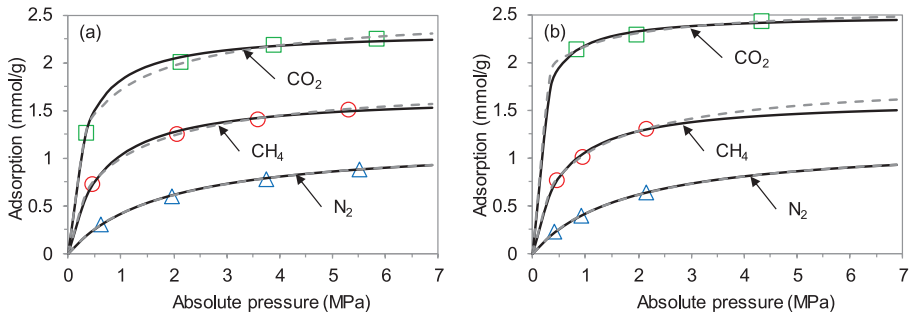

Figure 5. Best-fit curves for CO_2, CH_4 and N_2 adsorption (a) and desorption (b) with the Langmuir and D-R models (points = experimental data, black solid line = the Langmuir model and dashed line = the D-R model).

Table 2. Fitting parameters of the adsorption for CH_4, CO_2 and N_2 for the coal sample using the Langmuir and IAS (D-R) models.

Fit with the Langmuir model	Gas	Langmuir mole amount, N_L (mmol/g)		Langmuir pressure, P_L (kPa)	MSE* $(mmol/g)^2$
	CH_4	1.67		615.1	3.49×10^{-4}
	CO_2	2.33		283.9	7.78×10^{-4}
	N_2	1.17		1,793.2	3.49×10^{-5}
Fit with the D-R model	Gas	V_D (mmol/g)	D_i	P_s (kPa)	Absolute Error (mmol/g)
	CH_4	1.65	0.06245	17,052	2.51×10^{-5}
	CO_2	2.41	0.03715	20,670	3.17×10^{-4}
	N_2	1.02	0.10980	17,052	1.83×10^{-5}

*Mean squared error

Table 3. Fitting parameters of the desorption of CH_4, CO_2 and N2 for the coal sample using the Langmuir and IAS (D-R) models.

Fit with the Langmuir model	Gas	Langmuir mole amount, N_L (mmol/g)		Langmuir pressure, P_L (kPa)	MSE* $(mmol/g)^2$
	CH_4	1.61		520.1	1.91×10^{-4}
	CO_2	2.50		146.5	4.20×10^{-4}
	N_2	1.15		1,694	1.01×10^{-5}
Fit with the D-R model	Gas	V_D (mmol/g)	D_i	P_s (kPa)	Absolute Error (mmol/g)
	CH_4	1.69	0.06041	17,052	3.39×10^{-6}
	CO_2	2.53	0.01676	20,670	8.23×10^{-5}
	N_2	1.03	0.10923	17,052	8.44×10^{-6}

*Mean squared error

4.4.1. Comparison of adsorptions

The experimental and predicted gas adsorptions and the selectivity of binary and ternary mixed gas adsorption and desorption are shown in Figures 6-10.

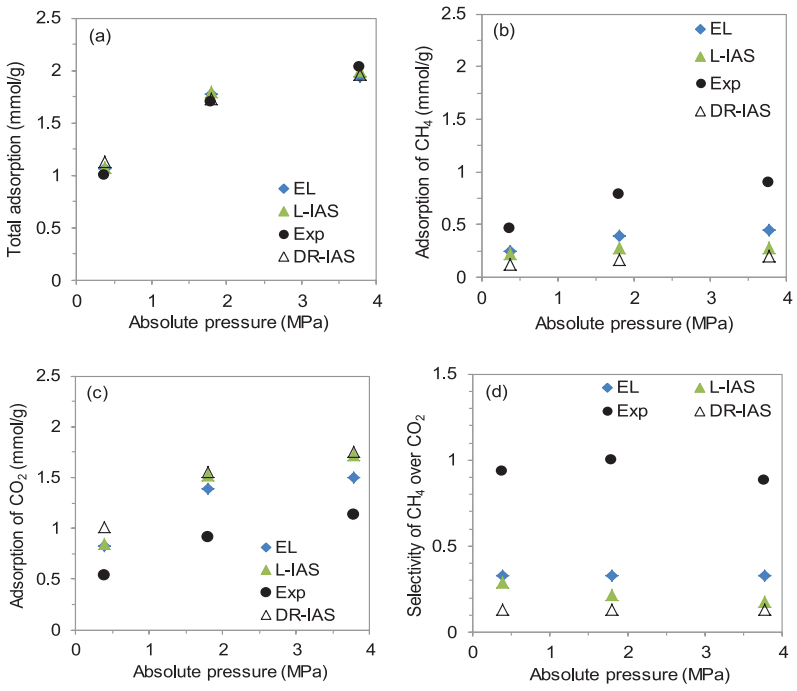

Figure 6. Adsorption and selectivity of mixed CH_4-CO_2. (a) total adsorption, (b) adsorption of CH_4, (c) adsorption of CO_2 and (d) selectivity of CH_4 over CO_2.

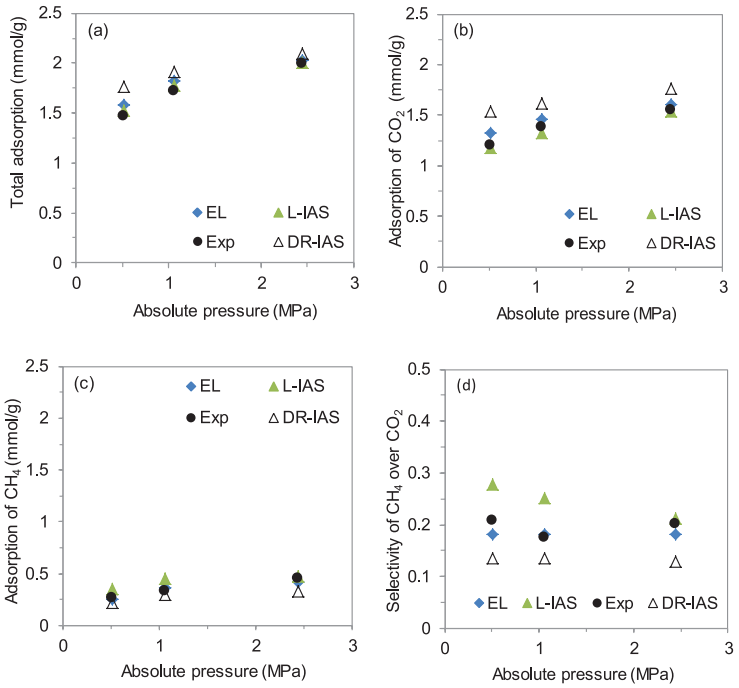

Figure 7. Desorption and selectivity of mixed CH_4-CO_2. (a) total adsorption, (b) adsorption of CH_4, (c) adsorption of CO_2 and (d) selectivity of CH_4 over CO_2.

For the binary gas adsorption, the results show that the total gas adsorptions predicted by the EL, L-IAS and D-R-IAS models are similar to the experimental results (Fig. 6a, Fig. 8a). The predicted CO_2 adsorption in the CO_2-CH_4 mixture (Fig. 6c) and CH_4 adsorption in the CH_4-N_2 mixture (Fig. 8b) are lower than the experimental measurements. This suggests that the counter components in the mixtures act reversely.

For the binary gas desorption, the results show that the total gas desorptions predicted by the EL, L-IAS and D-R-IAS models are similar to the experimental results for the CH_4-CO_2 mixture (Fig. 7a) but are lower than the experimental measurements for the CH_4-N_2 mixture (Fig. 9a). For the CH_4-CO_2 experiment, the predicted CH_4 adsorption by the L-IAS and EL models are similar to the experimental measurements (Fig. 7b) and predicted CO_2 adsorptions by the three models agree well with the experiments (Fig. 7c). For the CH_4-N_2 experiment, the predicted CH_4 adsorption by the three models are slightly lower than the experimental results (Fig. 9b) and predicted N_2 adsorptions by the three models are slightly higher than the experimental results (Fig. 9c).

For the ternary CH_4-CO_2-N_2 gas adsorption, the calculated total gas adsorptions using the EL and L-IAS models agree well with the experimental measurements (Fig. 10a). The calculated adsorptions of CO_2, N_2 and CH_4 using the D-R-IAS model are the closest to the experimental results (Figs. 10b through 10d).

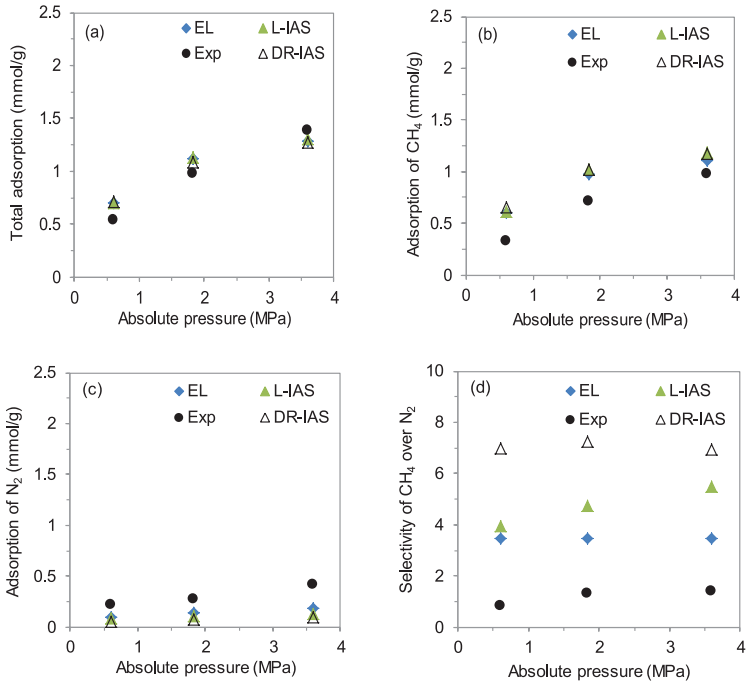

Figure 8. Adsorption and selectivity of mixed CH_4-N_2. (a) total adsorption, (b) adsorption of CH_4, (c) adsorption of N_2 and (d) selectivity of CH_4 over N_2.

4.4.2. Comparison of selectivity ratio

The selectivity ratio (or separation factor) of component *i* over component *j* is defined by John *et al*. (1985) as –

$$S_{i/j} = \frac{x_i / y_i}{x_j / y_j} \tag{24}$$

where *y* is the molar fraction of component *j* in the gas phase and *x* is the molar fraction of component *i* in the adsorbed phase.

For the binary CH_4-CO_2 adsorption, the experimental selectivity of CH_4 over CO_2 is about one. The predicted selectivity of CH_4 over CO_2 using the three models is lower than the experiment as shown in Figure 6d. This causes the predicted CH_4 adsorptions to be slightly lower than the experiments (Fig. 6b). For the binary CH_4-CO_2 desorption, the experimental selectivity of CH_4 over CO_2 is about 0.2 which is solely caused by the hysteresis of CO_2 desorption. The predicted selectivity from the EL model is quite similar to the experiment (Fig. 7d).

For the binary CH_4-N_2 adsorption, the predicted selectivity of CH_4 over N_2 is higher than the experiment which ranges from 0.8 to 1.3 (Fig. 8d). The overestimated

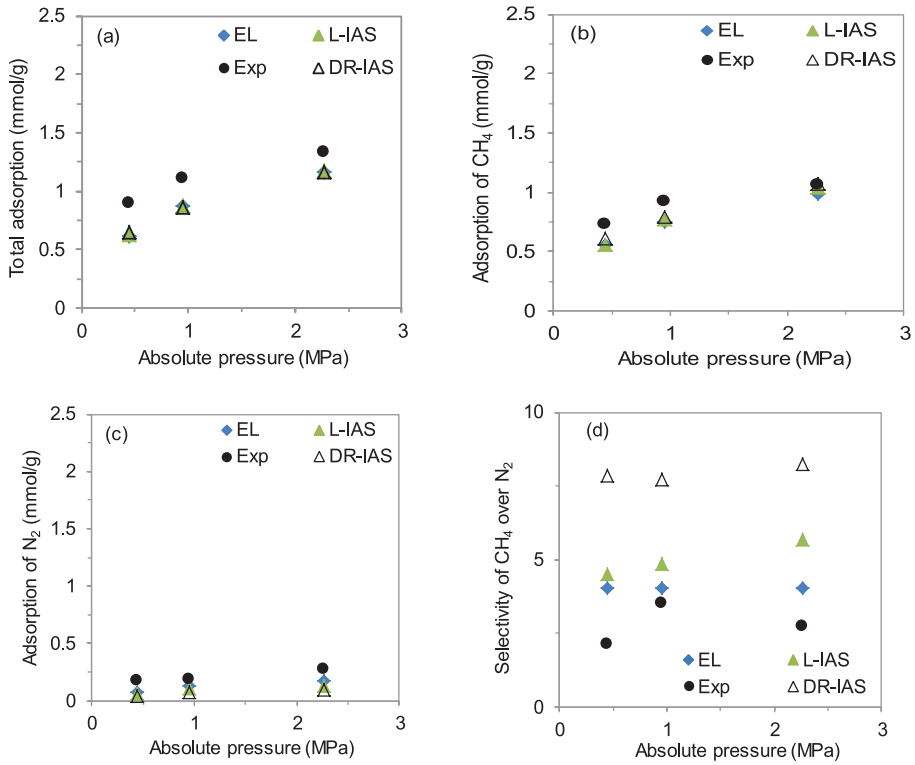

Figure 9. Desorption and selectivity of mixed CH_4-N_2. (a) total adsorption, (b) adsorption of CH_4, (c) adsorption of N_2 and (d) selectivity of CH_4 over N_2.

selectivity for CH_4 over N_2 makes the predicted CH_4 adsorption higher than the experiment (Fig. 8b). For the CH_4-N_2 desorption, the experimental selectivity of CH_4 over N_2 ranges from 2 to 4 which suggests that the adsorption ability of CH_4 is two to four times higher than that of N_2. The predicted selectivity by the EL model is similar but slightly higher than that obtained from the experiment (Fig. 9d).

For the ternary CH_4-CO_2-N_2 adsorption, the predicted selectivity of CH_4 over CO_2 by the L-IAS and EL models agrees well with the experimental data (Fig. 10e); the predicted selectivity of N_2 over CH_4 is similar to the prediction by the D-R-IAS model for a pressure of 2 MPa (Fig. 10f). The predicted selectivity of N_2 over CH_4 by the three models is all lower than the experimental data (Fig. 10g). Note that the mismatches between the predictions and the measurements might likely be caused by the contamination of N_2 in air when sampling and testing with GC.

5. CONCLUSIONS

We have presented the results of adsorption/desorption tests on coal samples taken from the Qinshui Basin, China. We used the volumetric adsorption measurement method for pure, binary and ternary gas adsorption and desorption. We interpreted

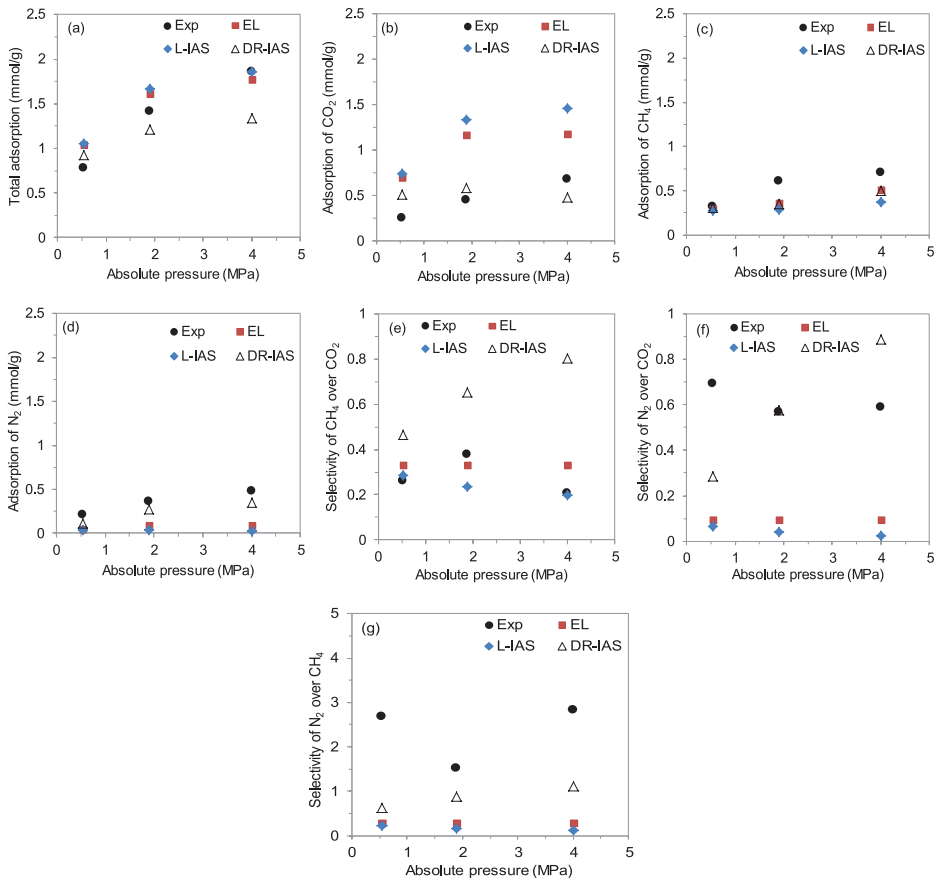

Figure 10. Adsorption and selectivity of mixed CO_2-CH_4-N_2. (a) total adsorption, (b) adsorption of CO_2, (c) adsorption of CH_4, (d) adsorption of N_2, (e) selectivity of CH_4 over CO_2, (f) selectivity of N_2 over CO_2 and (g) selectivity of N_2 over CH_4.

experimental observations using three isotherm models commonly reported in the literature. The following conclusions are drawn –

1. The pure gas adsorption is well predicted by the Langmuir and D-R models.
2. The adsorptions of N_2, CH_4 and CO_2 are found to have an approximate ratio of 1.0:1.3:2.4 for the study area in the basin. No significant hysteresis is observed for pure N_2 and CH_4 but CO_2 adsorption/desorption isotherms show a hysteresis. The binary and ternary adsorption tests show no large difference in sorption capacity but large difference during desorption.
3. The D-R model has a lower absolute error for fitting the experimental adsorption data for pure CH_4, CO_2 and N_2 compared to the Langmuir model.
4. The binary and ternary experiments show that there are significant hysteresis effects for mixture gases from adsorption to desorption.

5. The total adsorptions for binary and ternary gas mixtures predicted by the three models agree well with experimental observations. The predicted amount for low capacity adsorbate, however, is higher than the experimental data for the adsorption tests. The predicted amount of individual components has a fair match with the experimental data for the desorption tests.
6. The EL model appears to be the best in predicting the CO_2-CH_4 desorption while the D-R-IAS model predicts better the CO_2-CH_4-N_2 adsorption.

abbreviation

CH_4	=	Methane
N_2	=	Nitrogen
CO_2	=	Carbon dioxide
IAS	=	Ideal adsorbed solution
EL	=	Extended Langmuir
D-R	=	Dubinlin- Radushkevich
CBM	=	Coalbed methane
ECBM	=	Enhanced coalbed methane
GC	=	Gas chromatograph
RAS	=	Real adsorbed solution
RC	=	Reference cell
SC	=	Sample cell
SRK-EOS	=	Soave-Redlich-Kwong Equation of state
MSE	=	Mean squared error

ACKNOWLEDGEMENTS

The authors thank the financial support from Australia–China Joint Coordination Group on Clean Coal Technology Research & Development Grants, Department of Resources, Energy and Tourism, Australia. The Project was partially supported by the Fundamental Research Funds for the Central Universities, China University of Geosciences (Wuhan) (CUGL100249).

APPENDIX: SOAVE-REDLICH-KWONG EQUATIONS OF STATE

Soave (1972) brought forward a new equation of state based on Redlich and Kwong's work (1949). The equations are -

$$P = \frac{RT}{V-b} - \frac{a(T)}{V(V+b)} \tag{25}$$

$$a(T) = 0.42748 \frac{RT_c^2}{P_c}[1 + m(1 - T_r^{0.5})]^2 \tag{26}$$

$$b = 0.086640 \frac{RT_c}{P_c} \tag{27}$$

$$m = 0.48508 + 1.55171\omega - 0.15613\omega^2 \tag{28}$$

$$T_r = \frac{T}{T_c} \tag{29}$$

$$P_r = \frac{P}{P_c} \tag{30}$$

The SRK cubic equations for z are -

$$z^3 - z^2 + (A - B - B^2)z - AB = 0 \tag{31}$$

$$A = \frac{a(T) \cdot P}{(R \cdot T)^2} \tag{32}$$

$$B = \frac{b \cdot P}{R \cdot T} \tag{33}$$

In Eqs. 25 through 33, R is the universal gas constant of 8.314 J•mol^{-1}•K^{-1}, T_r and P_r are the reduced temperature and pressure in ˚K and Pa, respectively, T_c is the critical temperacture in K, P_c is the critical pressure in Pa and ω is the accentic factor. Eq. 31 was solved by using the Microsoft Excel solver to obtain the root with Visual Basic Applications codes.

REFERENCES

Battistutta E., Hemert V.P., Lutynski M., Bruining H. and Wolf K., 2010. Swelling and sorption experiments on Methane, Nitrogen and Carbon Dioxide on dry Selar Cornish coal. *International Journal of Coal Geology* **84(1)**, 39-48.

Clarkson C.R. and Bustin R.M., 2000. Binary gas adsorption/desorption isotherms: effect of moisture and coal composition upon carbon dioxide selectivity over methane. *International Journal of Coal Geology* **42(4)**, 241-271.

Connell L.D., Sander R., Pan Z., Camilleri M. and Heryanto D., 2011. History matching of enhanced coal bed methane laboratory core flood tests. *International Journal of Coal Geology* **87(2)**, 128-138.

Ding S.L., Zhu J.G., Baiping Zhen, Zhanyong Liu and Qinfu Liu, 2011. Characteristics of high rank coalbed methane reservoir from the Xiangning Mining Area, Eastern Ordos Basin, China. *Energy Exploration and Exploitation* **29(1)**, 33-48.

Dreisbach F., Staudt R. and Keller J.U., 1999. High pressure adsorption data of Methane, Nitrogen, Carbon Dioxide and their binary and ternary mixtures on activated carbon. *Adsorption* **5(3)**, 215-227.

Dutta P., Bhowmik S. and Das S., 2011. Methane and carbon dioxide sorption on a set of coals from India. *International Journal of Coal Geology* **85(3-4)**, 289-299.

Gamba G., Rota R., Storti G., Carra S. and Morbidelli M., 1989. Adsorption solution theory models for multicomponent adsorption equilibria. *AIChE Journal* **35(6)**, 959-966.

Goodman A.L., Busch A., Bustin R.M., Chikatamarla L., Day S., Duffy G.J., Fitzgerald J.E., Gasem K.A.M., Gensterblum Y., Hartman C., Jing C., Krooss B.M., Mohammed S., Pratt T., Robinson Jr R.L., Romanov V., Sakurovs R., Schroeder K. and White C.M., 2007. Inter-laboratory comparison II: CO_2 isotherms measured on moisture- equilibrated Argonne premium coals at 55 °C and up to 15 MPa. *International Journal of Coal Geology* **72(3-4)**, 153-164.

Gruszkiewicz S.M., Naney T.M., Blencoe G.J., Cole R.D., Pashin C.J. and Carroll E.R., 2009. Adsorption kinetics of CO_2, CH_4, and their equimolar mixture on coal from the Black Warrior Basin, West-Central Alabama. *International Journal of Coal Geology* **77(1-2)**, 23-33.

Hall F.E., Zhou C., Gasem K.M. and Robinson R.L., 1994. Adsorption of pure Methane, Nitrogen, and Carbon Dioxide and their binary mixtures on wet Fruitland coal. Society of Petroleum Engineers Paper 29194 presented at Society of Petroleum Engineers Eastern Regional Meeting. November 8-10 1994. Charleston, West Virginia, pp.329-343.

Hema S.J., Raj G.K. and Duane S.H., 2009. Shrinkage and swelling of coal induced by desorption and sorption of fluids: theoretical model and interpretation of a field project. *International Journal of Coal Geology* **77(1-2)**, 188-202.

Jessen K., Tang G-Q. and Kovscek A., 2008. Laboratory and simulation investigation of enhanced coalbed methane recovery by gas injection. *Transport in Porous Media* **73(2)**, 141-159.

John T.S., Benjamin M.C.T. and Ralph T.Y., 1985. Adsorption of gases on coals and heattreated coals at elevated temperature and pressure: 2. Adsorption from hydrogen-methane mixtures. *Fuel* **64(5)**, 621-626.

Joubert J.L., Grein C.T. and Bienstock D., 1973. Sorption of methane in moist coals. *Fuel* **52(3)**, 181-185.

Kelemen R.S. and Kwiatek M.L., 2009. Physical properties of selected block Argonne premium bituminous coal related to CO_2, CH_4, and N_2 adsorption. *International Journal of Coal Geology* **77(1-2)**, 2-9.

Majewska Z., Majewski S. and Zietek J., 2010. Swelling of coal induced by cyclic sorption/desorption of gas: experimental observations indicating changes in coal structure due to sorption of CO_2 and CH_4. *International Journal of Coal Geology* **83(4)**, 475-483.

Mazumder S., Karnik A. and Wolf K.H., 2006. Swelling of coal in response to CO_2 sequestration for ECBM and its effect on fracture permeability. *SPE Journal* **11(3)**, 390-398.

Mazumder S. and Wolf K.H., 2008. CO_2 and flue gas core food experiments for enhanced coalbed Methane. Society of Petroleum Engineers Paper 114790

presented at Society of Petroleum Engineers Asia Pacific Oil and Gas Conference and Exhibition, Perth, Australia, pp. 43.

Mitra A., Harpalani S. and Kumar A., 2008. CO_2/N_2 injection in deep coals and its impact on coal permeability. The 42nd U.S. Rock Mechanics Symposium (USRMS), American Rock Mechanics Association. San Francisco, CA.

Myers A.L. and Prausnitz J.M., 1965. Thermodynamics of mixed-gas adsorption. *AIChE journal* **11(1)**, 121-127.

O'Brien A.J. and Myers L.A., 1985. Rapid calculations of multicomponent adsorption equilibria from pure isotherm data. *Industrial & Engineering Chemistry Process Design and Development* **24(4)**, 1188-1191.

Papanicolaou C., Pasadakis N., Dimou D., Kalaitzidis S., Papazisimou S. and Foscolos E.A., 2009. Adsorption of NO, SO_2 and light hydrocarbons on activated Greek brown coals. *International Journal of Coal Geology* **77(3-4)**, 401-408.

Pini R., Ottiger S., Burlini L., Storti G. and Mazzotti M., 2010. Sorption of Carbon Dioxide, Methane and Nitrogen in dry coals at high pressure and moderate temperature. *International Journal of Greenhouse Gas Control* **4(1)**, 90-101.

Pini R., Ottiger S., Storti G. and Mazzotti M., 2009. Pure and competitive adsorption of CO_2, CH_4 and N_2 on coal for ECBM. *Energy Procedia* **1(1)**, 1705-1710.

Puri R. and Yee D., 1990. Enhanced coalbed Methane recovery. Society of Petroleum Engineers Paper 20732 presented at 65th Society of Petroleum Engineers Annual Technical Conference and Exhibition. September 23-26, 1990. New Orleans, Louisiana, pp. 10.

Redlich O. and Kwong J.N.S., 1949. On the thermodynamics of solutions. V: An equation of state. Fugacities of gaseous solutions. *Chemical Reviews* **44(1)**, 233-244.

Richter E., Schutz W. and Myers L.A., 1989. Effect of adsorption equation on prediction of multicomponent adsorption equilibria by the ideal adsorbed solution theory. *Chemical Engineering Science* **44(8)**, 1609-1616.

Schepers C.K., Oudinot Y.A. and Ripepi N., 2010. Enhanced gas recovery and CO_2 storage in Coalbed-Methane reservoirs: optimized injected-gas composition for mature basins of various coal rank. Society of Petroleum Engineers Paper 139723 presented at Society of Petroleum Engineers International Conference on CO_2 Capture. November 10-12, 2010. Stora, New Orleans, Louisiana, USA, pp. 21.

Shi J-Q. and Durucan S., 2005. A Model for changes in coalbed permeability during primary and enhanced Methane recovery. *Society of Petroleum Engineers Reservoir Evaluation & Engineering* **8(4)**, 291-299.

Soave G., 1972. Equilibrium constants from a modified Redlich-Kwong equation of state. *Chemical Engineering Science* **27(6)**, 1197-1203.

Stevens S.H. and Spector Denis, 1998. Advanced Resources International, Inc.; Riemer, Pierce, IEA Greenhouse Gas R&D Programme. 1998. Enhanced coalbed Methane recovery using CO_2 injection: worldwide resource and CO_2 sequestration potential. Society of Petroleum Engineers Paper 48881 presented

at Society of Petroleum Engineers International Oil and Gas Conference and Exhibition in China. November 2-6, 1998. Society of Petroleum Engineersctor Beijing, China, pp. 13.

Stevenson M.D., Pinczewski W.V., Somers M.L. and Bagio S.E., 1991. Adsorption/desorption of multicomponent gas mixtures at in-seam conditions. Society of Petroleum Engineers Paper 23026 presented at Society of Petroleum Engineers Asia-Pacific Conference Perth. Western Australia, pp. 741-756.

Sudibandriyo M., Pan Z., Fitzgerald J.E., Robinson R.L. and Gasem K.A.M., 2003. Adsorption of Methane, Nitrogen, Carbon Dioxide, and their binary mixtures on dry activated Carbon at 318.2 K and pressures up to 13.6 MPa. *Langmuir* **19(13)**, 5323-5331.

Talu O. and Zwiebel I., 1984. Multicomponent adsorption equilibria of nonideal mixtures. *AIChE journal* **32(8)**, 1263-1276.

Tang Q.G., Jessen K. and Kovscek R.A., 2005. Laboratory and simulation investigation of enhanced coalbed methane recovery by gas injection. *Springer Link* **73(2)**, 141-159.

Wang G.X., Wei X.R., Wang K., Massarotto P. and Rudolph V., 2010. Sorption-induced swelling/shrinkage and permeability of coal under stressed adsorption/desorption conditions. *International Journal of Coal Geology* **83(1)**, 46-54.

Wood G.O., 2002. Review and comparisons of D/R models of equilibrium adsorption of binary mixtures of organic vapors on activated carbons. *Carbon* **40(3)**, 231-239.

Yu H., Zhou L., Guo W., Cheng J. and Hu Q., 2008. Predictions of the adsorption equilibrium of methane/carbon dioxide binary gas on coals using Langmuir and ideal adsorbed solution theory under feed gas conditions. *International Journal of Coal Geology* **73(2)**, 115-129.

Zhou F., Allinson G., Wang J., Sun Q., Xiong D. and Cinar Y., 2012. Stochastic modelling of coalbed methane resources: A case study in Southeast Qinshui Basin, China. *International Journal of Coal Geology* **99**, 16-26.

Zhou F., Yao G., Tang Z. and Orodu O.D., 2011. Influence and sensitivity study of matrix shrinkage and swelling on enhanced coalbed methane production and CO_2 sequestration with mixed gas injection. *Energy Exploration & Exploitation* **29(6)**, 759-776.